Food Control 29 (2013) 461–470

Contents lists available at SciVerse ScienceDirect

Food Control

journal homepage: www.elsevier.com/locate/foodcont

A comparison of Raman and FT-IR spectroscopy for the prediction of meat spoilage

Anthoula A. Argyri [a,*], Roger M. Jarvis [b], David Wedge [b], Yun Xu [b], Efstathios Z. Panagou [a], Royston Goodacre [b], George-John E. Nychas [a]

[a] Lab of Microbiology and Biotechnology of Foods, Dept. of Food Science and Technology, Agricultural University of Athens, Iera Odos 75, Athens 11855, Greece
[b] School of Chemistry and Manchester Interdisciplinary Biocentre, University of Manchester, 131 Princess Street, Manchester, M1 7DN, UK

ARTICLE INFO

Article history:
Received 8 December 2011
Received in revised form
25 April 2012
Accepted 16 May 2012

Keywords:
Meat spoilage
Raman spectroscopy
FT-IR
Multivariate analysis
Evolutionary computing

ABSTRACT

In this study, time series spectroscopic, microbiological and sensory analysis data were obtained from minced beef samples stored under different packaging conditions (aerobic and modified atmosphere packaging) at 5 °C. These data were analyzed using machine learning and evolutionary computing methods, including partial least square regression (PLS-R), genetic programming (GP), genetic algorithm (GA), artificial neural networks (ANNs) and support vector machines regression (SVR) including different kernel functions [i.e. linear (SVR_L), polynomial (SVR_P), radial basis (RBF) (SVR_R) and sigmoid functions (SVR_S)]. Models predictive of the microbiological load and sensory assessment were calculated using these methods and the relative performance compared. In general, it was observed that for both FT-IR and Raman calibration models, better predictions were obtained for TVC, LAB and *Enterobacteriaceae*, whilst the FT-IR models performed in general slightly better in predicting the microbial counts compared to the Raman models. Additionally, regarding the predictions of the microbial counts the multivariate methods (SVM, PLS) that had similar performances gave better predictions compared to the evolutionary ones (GA-GP, GA-ANN, GP). On the other hand, the GA-GP model performed better from the others in predicting the sensory scores using the FT-IR data, whilst the GA-ANN model performed better in predicting the sensory scores using the Raman data. The results of this study demonstrate for the first time that Raman spectroscopy as well as FT-IR spectroscopy can be used reliably and accurately for the rapid assessment of meat spoilage.

1. Introduction

Evaluation of the degree of meat spoilage and/or hygiene level is usually made either subjectively based on qualitative criteria or by time consuming, destructive microbiological analyses that do not provide the 'immediate answer required' (McMeekin, Mellefont, & Ross, 2007, Nychas, Skandamis, Tassou, & Koutsoumanis, 2008). To complement these approaches, the meat industry needs rapid analytical procedures to define and quantify spoilage indicators, in order to both determine suitable processing methods for the raw material, and to predict the remaining shelf life of the product. For example, it would be desirable to develop an automated, reproducible and quantitative approach defining the spoilage state of a product objectively. At present, there is no consensus as to what indicators are representative of the early signs of incipient spoilage for meat, and the changes in the technology of meat preservation (e.g. vacuum, modified atmosphere, etc.) makes it all the more difficult to evaluate spoilage objectively. This is true for both retailers and wholesalers of fresh meat products, where valid methodologies to ensure the freshness and safety of their products are paramount, whilst inspection authorities need reliable methods for control purposes.

Recently, some interesting mathematical approaches have been applied to describe the kinetics of ephemeral/specific spoilage organisms (E(S)SO) with the aim of predicting the spoilage of various foods (McMeekin et al., 2006). Other approaches are based on the use of biosensors (enzymatic reactor systems), electronic noses (arrays of sensors), and vibrational spectroscopy methods (e.g., FT-IR, Raman spectroscopy) (Ellis, Broadhurst, Clarke, & Goodacre, 2005; Herrero, 2008a) for the same purpose. In particular, Fourier transform infrared (FT-IR) spectroscopy has attracted considerable interest since it is rapid and non-destructive and has been identified as having considerable potential for applications in food and related industries, with several reports on muscle food analysis (van Kempen, 2001). Al-Jowder, Defernez, Kemsley, and

* Corresponding author. Fax: +30 210 529 4693.
E-mail address: aargyri@aua.gr (A.A. Argyri).

0956-7135/$ – see front matter © 2012 Elsevier Ltd. All rights reserved.
doi:10.1016/j.foodcont.2012.05.040

Wilson (1999) and Al-Jowder, Kemsley, and Wilsonb (1997) reported that mid-infrared spectroscopy with attenuated total reflectance (FT-IR-ATR) has the potential to be established as a technique for meat authentication, whilst Yang and Irudayaraj (2001) demonstrated the dynamics of FT-IR-ATR and FT-IR-PAS (photoacoustic spectroscopy) techniques for beef and pork quality control through a multi-layer analysis. In addition, according to Karoui et al. (2007), FT-IR-ATR can be adapted for online detection of freeze–thawed fish from fresh fish samples. Finally, studies correlating the microbial spoilage of meat with biochemical changes within the meat substrate have been conducted for chicken (Ellis, Broadhurst, Kell, Rowland, & Goodacre, 2002) and beef tissues (Ellis, Broadhurst, & Goodacre, 2004) that were ground to a paste and stored aerobically at ambient temperature. More recent studies of this type correlate the spoilage status (microbial counts and sensory scores) of beef and pork stored under different conditions (i.e. temperature and packaging) with the biochemical fingerprints observed with FT-IR spectroscopy (Ammor, Argyri, & Nychas, 2009; Argyri, Panagou, Tarantilis, Polysiou, & Nychas, 2010; Papadopoulou, Panagou, Tassou, & Nychas, 2011). Moreover, metabolic fingerprinting using FT-IR has been shown to correlate very well with the bacterial counts of other foods, such as milk during storage (Nicolaou & Goodacre, 2008; Nicolaou, Xu, & Goodacre, 2011).

Raman spectroscopy is also a vibrational spectroscopy method that is complementary to infrared absorbance. Raman spectroscopy has the advantage over FT-IR that the contribution from water is very small (since H_2O is a weak Raman scatterer) and so can be used directly on the food without recourse to ATR. Raman spectroscopy has attracted increasing interest as a versatile and rapid tool for analysis of biological samples, and potential applications have been found in areas ranging from medical diagnostics and tissue or organism characterization, to analysis of food and agricultural products. As with FT-IR, Raman spectroscopy can be used in food analysis, since it is non-destructive, requires little pre-treatment of samples and provides information about different food compounds at the same time, offering quantitative analysis of food components with simultaneous information on molecular structure. In comparison to FT-IR, smaller portions of sample are required and instrumentation can be less expensive and portable. Examples of this technique for muscle food analysis, include studies upon the authenticity of poultry species (Ellis et al., 2005), the sensory quality of beef (Beattie, Bell, Farmer, Moss, & Desmond, 2004), the structural changes in fish proteins (Herrero, Carmona, & Careche, 2004) and quality screening of fish (Marquardt & Wold, 2004), as well as changes in pork proteins (Böcker et al., 2007) and the texture of pork muscle (Herrero, 2008b). The only reported study in meat spoilage using Raman spectroscopy refers to Raman measurements on pork during storage, without parallel measurements of microbial counts and/or sensory scores and subsequent correlation of the latter with the Raman spectra (Sowoidnich et al., 2010). However, in a recent study (Nicolaou et al., 2011), Raman and FT-IR spectroscopy were applied to detect and enumerate the bacterial counts of certain microbial groups growing in milk.

In many industrial (spectroscopic) applications, Partial Least Squares (PLS) is used to make regression models because of its simplicity to use, speed, relative good performance and easy accessibility. However, nonlinear relations can only be modelled in a limited way (i.e., weak nonlinearities) by taking into account more latent variables (Thissen, Ustun, Melssen, & Buydens, 2004). Often artificial neural networks (ANNs) are used and are considered to be good nonlinear regression methods for the treatment of spectral data (Blanco & Pages, 2002; Despagne, Massart, & Chabot, 2000). Support Vector Machines (SVMs), originally proposed by Vapnik et al. in 1995, might also be used for spectral regression purposes (which then is called support vector regression: SVR). A possible large advantage of SVR is its ability to model nonlinear relations and it is gaining popularity due to its attractive features and promising empirical performance (Shinoda et al., 2008; Thissen et al., 2004). SVM is a new type of machine learning theory based on statistical learning theory, that emphasizes statistical learning in the case of fewer samples. The structural risk minimization principle derived from statistical learning theory takes this as the foundation, as compared with ANNs, giving the SVMs prominent advantages. First, the strong theoretical basis provides high generalization capability and avoids overfitting. Second, the global model is capable of dealing efficiently with high-dimensional input vectors. Third, the solution is sparse and only a subset of training samples contributes to this solution, thereby reducing the workload (Zou, Dou, Mi, Zou, & Ren, 2006).

Evolutionary algorithms (EAs) are the common term used for algorithms based on principles of natural evolution. EAs contain genetic algorithms (GAs), evolution strategies, evolutionary programming and genetic programming (GP). GAs are optimization tools and randomized search techniques guide by the principles of evolution and natural genetics (Guo et al., 2000). They have been proved to be an efficient method in the feature selection problems and they require no knowledge or gradient information about the response surface and can be employed for a wide variety of optimization problem (Konoz & Golmohammadi, 2008). The solution produced by GP emerges as a result of Darwinian natural selection and genetic crossover (sexual recombination) in a population of computer programs (Goodacre, 2005; Tang & Li, 2002). Since the GA is an algorithm based on evolutionary computation and survival of the fittest, it is often applied to optimization problems such as optimizing the free variables in a hypothesis function, the network architecture and its weights for ANNs (Ferentinos, 2005; Shinoda et al., 2008; Torres, Hervás, & Amador, 2005).

The aim of this study was to investigate and compare the dynamics of FT-IR and Raman spectroscopy in predicting the microbial spoilage of meat stored under different packaging conditions (aerobic and modified atmosphere packaging) at 5 °C. Time series spectroscopic, microbiological and sensory analysis data were obtained from minced beef samples and analyzed using machine learning and evolutionary computing methods, including partial least square regression (PLS-R), genetic programming (GP), artificial neural networks (ANNs) and support vector machines regression (SVR). Models predictive of the microbiological load and sensory assessment were calculated using these methods and the relative performances compared. The results demonstrate that Raman spectroscopy as well as FT-IR spectroscopy can be applied reliably and accurately to the assessment of meat spoilage. A part of this work was published in the proceedings of 7ICPMF (Argyri et al., 2011).

2. Materials and methods

2.1. Preparation of the minced beef samples

Fresh minced beef of 2 different batches (approximately 10 kg) at normal pH (pH 5.5) was obtained from a retail market in Athens (Greece) and transported under refrigeration to the laboratory within 30 min, where it was held at 1 °C for 1–2 h. Two portions of 75 g were placed onto styrofoam trays. These samples were packaged under two packaging conditions, air and MAP (40% CO_2/30% O_2/30% N_2), and stored at 5 °C. For the aerobic storage, the samples were placed into permeable polyethylene bags for domestic use. For the MAP the samples were packed into plastic pouches (200 mm wide − 240 mm long − 90 μm thickness), of gas permeability at 20 °C and 50% relative humidity of ca. 25, 90 and 6 cm^3/m^2

per day/10^5 Pa for CO_2, O_2 and N_2, respectively, using a HenkoVac 1900 Machine. The samples were divided according to their origin from the 2 different meat batches, stored in different thermostatic champers and were considered as different biological replicates. The minced beef samples were stored for 144 h (6 d) aerobically and under MAP at 5 °C, until spoilage was pronounced, whilst a total of 13 sampling points were collected for each condition with a sampling frequency of 12 h. At each time point, 2 packages were opened for each packaging condition and from each package one portion was used for microbiological analysis, FT-IR and Raman spectroscopy measurements and the other one was used for sensory analysis. Microbiological and sensory analyses, pH measurements, FT-IR and Raman spectroscopy measurements were carried out in an attempt to correlate the total and individual microbial loads from these samples with the biochemical metabolites that fluctuate during the spoilage process.

2.2. Microbiological analysis

For microbiological analysis 25 g of meat sample were added to 225 ml of sterile quarter strength Ringer's solution (LAB M) and homogenized in a stomacher (Lab Blender) for 60 s at room temperature. Serial decimal dilutions in quarter strength Ringer's solution were prepared and 1 or 0.1 ml samples of appropriate dilutions were poured or spread in triplicates on non-selective and selective agar plates. Growth media were used as follows: total viable counts were determined on Tryptic Glucose Yeast Agar (402145, Biolife, Milan, Italy), incubated at 30 °C for 48 h; lactic acid bacteria on MRS agar (401728, Biolife, Milan, Italy) (pH = 5.7) overlaid with the same medium and incubated at 30 °C for 72 h; *Brochothrix thermosphacta* on STA Agar Base (402079 supplemented with selective supplement 4240052, Biolife, Milan, Italy), incubated at 25 °C for 48 h; *Enterobacteriaceae* on Violet Red Bile Glucose Agar (402188, Biolife, Milan, Italy) overlayed with the same medium and incubated at 37 °C for 24 h; yeasts on Rose Bengal Chloramphenicol Agar Base (LAB 36 supplemented with selective supplement X009, LAB M, UK), incubated at 25 °C for 72 h; *Pseudomonas* spp. on Pseudomonas Agar Base (CM559 supplemented with selective supplement SR103, Oxoid, Basingstoke, UK), incubated at 25 °C for 48 h.

Data analysis of microbial counts; The growth data (log cfu g^{-1}) of the different spoilage bacteria of minced meat were modelled as a function of time using the primary model of Baranyi and Roberts (1994), and the kinetic parameters of maximum specific growth rate (μ_{max}) and lag phase (lag) were estimated. For curve fitting the Institute of Food Research program DMFit, was used, which was kindly provided by Dr. J. Baranyi (Institute of Food Research, Norwich, United Kingdom).

2.3. pH measurement

The pH value was recorded by a pH metre (Metrohm 691 pH metre), with the glass electrode being immersed in the homogenate of minced meat following microbiological analysis.

2.4. Sensory analysis

Sensory evaluation of meat samples was performed during storage according to Gill and Jeremiah (1991) by a sensory panel composed of five trained staff members from the laboratory. The same individuals participated in each evaluation, which was conducted blind. The sensory evaluation was carried out in artificial light and the temperature of packaged product was similar to ambient temperature. The colour and odour were described before and after cooking (20 min at 180 °C in preheated oven), whereas taste was described after cooking. Odour characteristics of minced beef, as determined by special samples kept frozen and thawed prior to each sensory evaluation, were considered as fresh. Putrid, sweet, sour, or cheesy odours were regarded as indicative of microbial spoilage and such samples were classified as spoiled. Bright colours typical of fresh oxygenated meat were considered indicative of fresh meat, whereas a persistent dull or unusual colour rendered the sample spoiled. Each attribute was scored on a three-point hedonic scale where: 1 = fresh; 2 = marginal; and 3 = unacceptable. A score of 1.5 was used to characterize a sample as semi-fresh and was the first indication of change from that of typical fresh meat (i.e., less vivid red colour, odour and flavour slightly changed, but still acceptable by the consumer). Scores above 2 rendered the product spoiled and indicated the end of the product's shelf life.

2.5. FT-IR spectroscopy

FT-IR analysis was performed using a ZnSe 45° ATR (attenuated total reflectance) crystal with a Smart ARK accessory on a Nicolet 6700 FT-IR Spectrometer equipped with a DLaTGS detector with KBr Window. The samples were placed on the ZnSe ATR crystal so that the aerobic upper surface of the meat was held in intimate contact with the crystal. The sample then was pressed with a gripper so as to have the best possible contact with the crystal. The spectrometer was programmed with Omnic Software-version 7.3 to collect spectra over the wavenumber range 4000 to 650 cm^{-1}, the scans per measurement were 100 resulting in a total integration time of 2 min. The ZnSe ATR crystal was capable of 12 external reflections, with the evanescent field affecting a depth of 1.01 μm. Reference spectra were acquired by collecting a spectrum from the cleaned blank crystal prior to the presentation of each sample replicate. At the end of each sampling, the crystal surface was first cleaned with detergent, washed with distilled water, dried with lint-free tissue, then cleaned with analytical grade ethanol and finally dried with lint-free tissue at the end of each sampling interval. Two (2) replicate FT-IR spectra were collected from each of the 2 biological replicate samples. The number of FT-IR spectra collected was 98. Although the FT-IR spectra were collected over the wavenumber range 4000 to 650 cm^{-1}, the range that was used for further analysis was between 1800 and 900 cm^{-1}.

2.6. Raman spectroscopy

A 633 nm DeltaNu Advantage probe with a right-angled sampling attachment was used for data collection, with the aperture positioned 16 mm above the surface of the compressed meat sample delivering ~6 mW laser power. Spectra were acquired over a Stokes Raman shift range of 200 to 3400 cm^{-1} at a medium resolution of 6 cm^{-1}. Each spectrum was integrated for 60 s and the spectra exported from the DeltaNu control software as ASCII-XY files for subsequent numerical analysis. Five (5) replicate Raman spectra were collected from each of the 2 biological replicate samples, from randomly selected positions on the sample surface. The number of spectra collected was 260.

2.7. Modelling of the spectral data

2.7.1. Preprocessing

Prior to data analysis, the FT-IR and Raman spectra were background corrected using the standard normal variate (SNV) transformation. This approach was selected on a purely empirical basis with respect to the prediction errors calculated from the regression algorithms.

2.7.2. Partial least squares regression (PLS-R)

PLS is one of the most commonly used multivariate linear regression methods which works on the basis of extracting a small number of orthogonal latent components (A) that are linear combinations of the original ($\boldsymbol{X}$). Using extracted latent components instead of raw variables, PLS can efficiently analyse the data with more variables than samples such as FT-IR or Raman spectra. The complexity of the PLS-R model is determined by the number of the latent components been extracted from the data and this is determined by using a leave-one-out cross-validation (LOO-CV) procedure on the training set only. The number of latent components needed to yield the best root mean square error (RMSE) of the cross-validation is chosen for the modelling.

2.7.3. Support vector machines regression

Support vector machines (SVM) is a relatively new tool, originally designed for classification problems involving large multidimensional data sets. There are two distinctive features in SVM, one is to solve both linear and nonlinear classification/regression problem using the same methodology. In SVM, all nonlinear problems are transferred to linear by mapping the data $\boldsymbol{X}$ into a high-dimensional feature space via a nonlinear mapping function (kernel function) and perform a linear classification or regression in this feature space. The dimensionality of the feature space is determined by the choice of kernel function and its parameters while the complexity of the model is determined by an extra penalty parameter. Another feature in SVM is that the model produced only uses a subset of the training data which is named support vectors. In SVR samples within the model prediction accuracy, which is defined by an external parameter, were ignored and only those having significant leverage to the model, i.e. support vectors, will have their contributions to the modelling. This methodology, in theory, can give a better generalization performance of the model. An excellent review of SVR can be found in Smola and Schölkopf (2004).

In this study, different kernel functions including linear (SVR_L), polynomial (SVR_P), radial basis function (RBF) (SVR_R) and sigmoid functions (SVR_S), were tested for their capability on fitting Raman and FT-IR data. Similar to the PLS-R modelling the different SVM parameters needed for each model were also optimized by using LOO-CV on the training set in terms of RMSE.

2.7.4. Genetic programming, genetic algorithm and artificial neural network analyses

Three different machine learning techniques were also used for bacterial predictions from the spectroscopic data, namely:

i) **Genetic Programming (GP)**; GP involves the generation of a number of random solutions, each of which is a multi-component function, structured as a tree-based structure. These solutions are 'evolved' through a process imitative of natural selection (Koza, 1992). A population of 250 solutions was evolved for up to 500 generations. 1/3 of the training data were held back as a validation set and evolution was stopped when no improvement in the validation fitness (mean square error) had been observed for 25 generations. 100 runs were carried out and the solution with the best R^2 value on the training data was selected.

ii) **Genetic Algorithm (GA) selecting GP**; Genetic Programming should automatically select the 'best' inputs to use. However, when there are a large number of inputs (as in this study), the search space is very large and can be difficult to search satisfactorily. In this method a GA (Goldberg, 1989) was used to select which inputs to use within a GP. GAs use bit-strings, in this case representing inclusion (1) or exclusion (0) of each variable. As with GPs, GAs may be evolved over a number of generations. In this study a population of 50 randomly selected inputs was evolved for 10 generations. For each selection of inputs, 3 GPs were evolved and the fitness of this selection of inputs was assigned the value of the median R^2 value. After 10 generations, the selection of inputs with the best R^2 value was considered to be the best. 100 GP runs were then carried out as described in the last section, but only using the selected inputs.

iii) **GA selecting Artificial Neural Network (ANN)** Again, a GA was used to select inputs prior to ANN analysis. ANNs model nonlinear relationships via a multi-layer structure of computational 'neurons', each connected in parallel to all neurons in the layer below. ANNs are 'trained' by iteratively adjusting weights which mediate the signals passing between neurons in order to reduce the discrepancy between the target and actual output of the neuron in the bottom layer (Haykin, 2009). The ANNs used here contained an input layer, a single hidden layer and a single output neuron. The hidden layer neurons had sigmoidal transfer functions and the output neuron had a linear transfer function. The number of hidden layer neurons was selected using 4 additional bits in the GA bit-string, resulting in between 1 and 16 neurons. Each ANN was trained for up to 1000 generations, again with early stopping if the validation MSE showed no improvement for 25 epochs. Again, 3 ANNs were trained for each selection of inputs, and at the end of the GA, the best inputs were used to train 100 ANNs.

2.7.5. Model validation

All the methods used in this paper are supervised techniques; i.e., they use *a priori* knowledge of the solution to a problem. In order to optimize calibration, it is important to include a set of validation data against which to select the optimal number of latent variables.

To test the validity of the supervised models described above, the data were partitioned into model calibration and test sets. More specifically, the data (counts of all the microbial groups, sensory scores, FT-IR and Raman spectra) were divided in two parts regarding the different biological replicates for each sampling time. One of these data sets was used for the calibration, i.e. building the model and the other was used for the validation of the models. The FT-IR data set consisted of 98 spectra (469 variables), whilst the Raman total data set consisted of 260 spectra (1024 variables), with their corresponding microbial counts and sensory scores.

2.7.6. Performance of the models

The criteria for evaluating and comparing the models were the RMSE and the square of the correlation coefficient R^2 for the known values versus validation predictions for both the viable counts and the sensory scores. In addition, the percentage of Prediction Error (% PE) was used for the viable counts whilst the confusion matrix was used to evaluate the correct classification of the predicted sensory scores.

Prediction errors (PE, in $\log_{10}$) or residuals for individual prediction cases were calculated as

$$\mathrm{PE} = O - P \tag{1}$$

where O is the observed value (log), P is the predicted value (log), $\mathrm{PE} < 0$ are fail-safe predictions, and $\mathrm{PE} > 0$ are fail-dangerous predictions. Median PE served as a measure of prediction bias, and median absolute PE served as a measure of prediction accuracy.

To determine whether individual prediction errors were acceptable, we used a prediction zone (APZ) (Oscar, 2009);

$$-1.0 \log < \text{acceptable PE} < 0.5 \log \quad (2)$$

where the APZ was twice as wide in the fail-safe direction because greater error can be tolerated in the fail-safe direction when a model is used to predict food safety (Oscar, 2009).

The percentage of PE (% PE) in the APZ served as an overall measure of model performance:

$$\%PE = \left(\frac{PE_{in}}{PE_{total}}\right) \times 100 \quad (3)$$

where PE_{in} is the number of PE in the APZ, and PE_{total} is the total number of PE in the evaluation. A % PE of >70% indicated a simulation model that provided acceptable predictions for the test data set (Oscar, 2005).

In this work, a 2 step approach was followed to predict the sensory scores. Regression was applied as a 1st step to predict all these stages of spoilage (1, 1.5, 2, 2.5, 3) as assessed from sensory analysis, thereby using a near continuous scale. In a 2nd step (classification), each predicted sensory score was rounded to the closest class membership, in order to aid interpretability of the results. More precisely, the confusion matrix for the sensory scores was derived using a 0.25 cut-off value for predicted values with respect to the closest sensory value. For example, a sample with a predicted score of 1.35 was classified as 1.5. Samples with a score of 1 were categorised as fresh, samples scoring 1.5 were categorised as semi-fresh and scores above 2 that pointed the end of the products' shelf life were categorised as spoiled. Finally, the accuracy of the model was visualized with the % recognition rate. A similar approach was followed in previous work (Argyri et al., 2010).

3. Results and discussion

3.1. Microbial association and shelf life

The microbiological analysis revealed that initial flora of the minced beef consisted of *Pseudomonas* spp., *Br. thermosphacta*, *Enterobacteriaceae*, lactic acid bacteria (LAB), yeasts and moulds. During the aerobic storage of minced beef, *Pseudomonas* spp. were the dominant microorganisms, followed by *Br. thermosphacta*, yeasts and moulds, LAB and *Enterobacteriaceae* (Fig. 1). Packaging under MAP delayed the growth of the pseudomonads, yeasts and moulds, and *Enterobacteriaceae* and suppressed the maximum level of the aerobic counts compared with the aerobic storage, but it affected positively the growth of *Br. thermosphacta* and LAB (Fig. 1; Table 1). Similar results for meat have been described previously (Ellis & Goodacre, 2001; Ercolini, Russo, Torrieri, Masi, & Villani, 2006; Sakala et al., 2002; Skandamis & Nychas, 2001, 2002; Tsigarida, Skandamis, & Nychas, 2000).

The sensory evaluation of the mince defined the end of shelf life at 60 h for aerobic storage and 72 h for storage under MAP (Fig. 1). The type of muscle spoilage under aerobic conditions was characterized by putrefaction, which is related to proteolytic activity and off odour production by the dominant Gram-negative bacteria (Nychas, Drosinos, & Board, 1998). In the case of MAP the spoilage was characterized by muscle souring, of which the main causes, if not the most important, are LAB and *Br. thermosphacta*.

The pH values at the beginning of storage were within the normal range for fresh beef (Borch, Kant-Muemans, & Blixt, 1996), with the initial mean value of 5.75. There was a decrease in pH for all samples stored under MAP in relation to storage time, whilst an increase was observed in pH values of all samples stored aerobically. The final mean pH values for aerobic storage and storage under MAP were 6.11 and 5.60 respectively.

Table 1 summarizes the estimates by the primary model of Baranyi and Roberts (1994) for the final population, lag phase and maximum specific growth rate for the total viable counts (TVC), pseudomonads, *Br. thermosphacta*, *Enterobacteriaceae*, LAB, yeasts and moulds for each of the packaging condition tested, whilst Fig. 1 shows the growth curves of all the above microorganisms as well as the sensory scores.

3.2. FT-IR and Raman spectroscopy

Typical spectral data obtained from FT-IR in the range of 1800 to 900 cm^{-1} and Raman in the range of 3400 to 200 cm^{-1} collected from minced beef stored aerobically and under MAP at 5 °C are shown in Figs. 2 and 3 respectively.

3.3. Calibration models

Tables 2 and 3 present the RMSE and the R^2 values for the models built for FT-IR and Raman measurements. In general, it was observed that for both FT-IR and Raman calibration models, better

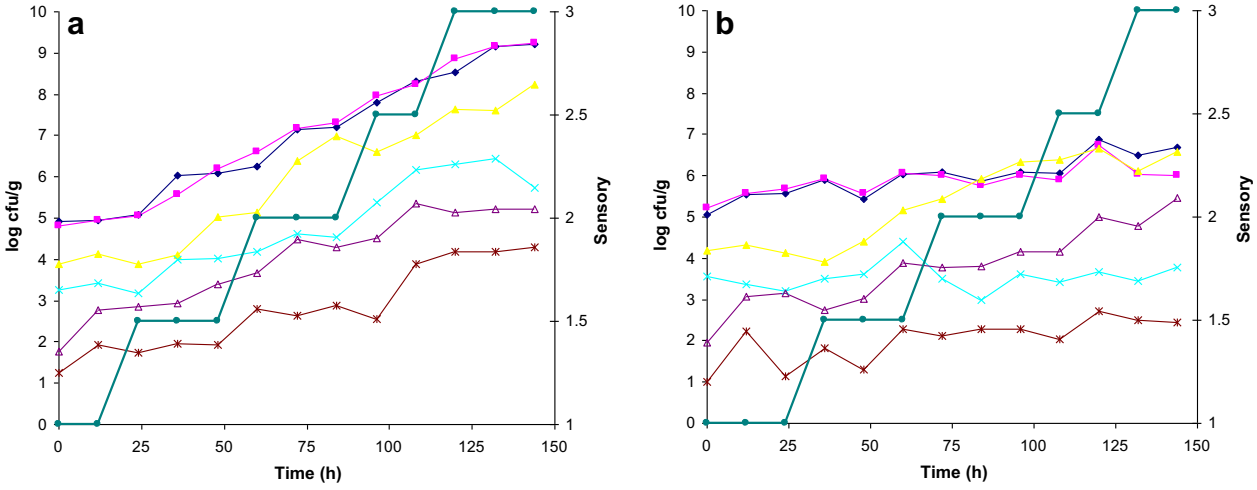

Fig. 1. Growth curves of all the tested microbial groups (primary axis) and sensory scores (secondary axis) for the minced beef stored aerobically (a) and under MAP (b) at 5 °C; (♦) Total Viable Counts, (■) pseudomonads, (▲) *Br. thermosphacta*, (X) yeasts and moulds, (△) LAB, (✻) Enterobacteriaceae, (●) Sensory scores.

Table 1
Kinetic parameters of the microbial association of meat estimated by the primary model of Baranyi and Roberts (1994).

Temperature (°C)	Microorganisms	Initial population (log cfu/cm^2)	Final population (log cfu/cm^2)	μ_{max}	lag	R^2
Air	TVC	4.91 ± 0.17[a]	∞[b](9.22)[c]	0.078 ± 0.005	8.99 ± 0.93	0.98
	Pseudomonads	4.80 ± 0.09	∞ (9.23)	0.082 ± 0.004	12.66 ± 1.90	0.96
	Br.thermosphacta	3.89 ± 0.12	∞ (8.24)	0.083 ± 0.005	21.55 ± 2.43	0.94
	Yeasts-Moulds	3.25 ± 0.03	6.19 ± 0.16 (5.74)	0.091 ± 0.019	43.69 ± 9.92	0.92
	LAB	1.78 ± 0.03	5.28 ± 0.16 (5.22)	0.068 ± 0.014	1.39 ± 0.29	0.94
	Enterobacteriaceae	1.24 ± 0.09	∞ (4.29)	0.059 ± 0.011	30.12 ± 7.02	0.85
MAP	TVC	5.05 ± 0.08	∞ (6.68)	0.026 ± 0.009	43.56 ± 8.52	0.67
	Pseudomonads	5.21 ± 0.03	∞ (6.00)	0.016 ± 0.004	30.90 ± 6.27	0.52
	Br.thermosphacta	4.18 ± 0.07	6.44 ± 0.11 (6.57)	0.106 ± 0.029	42.60 ± 7.12	0.92
	Yeasts-Moulds	3.57 ± 0.11	∞ (3.77)	0.008 ± 0.003	23.28 ± 6.03	0.42
	LAB	1.95 ± 0.07	∞ (5.47)	0.051 ± 0.004	–	0.94
	Enterobacteriaceae	1.00 ± 0.15	∞ (2.43)	0.030 ± 0.004	13.68 ± 3.03	0.80

[a] Standard error.
[b] Estimated by the Baranyi model. ∞ Fitted curve was completed without upper asymptote (semisegmoidal).
[c] Determined experimentally.

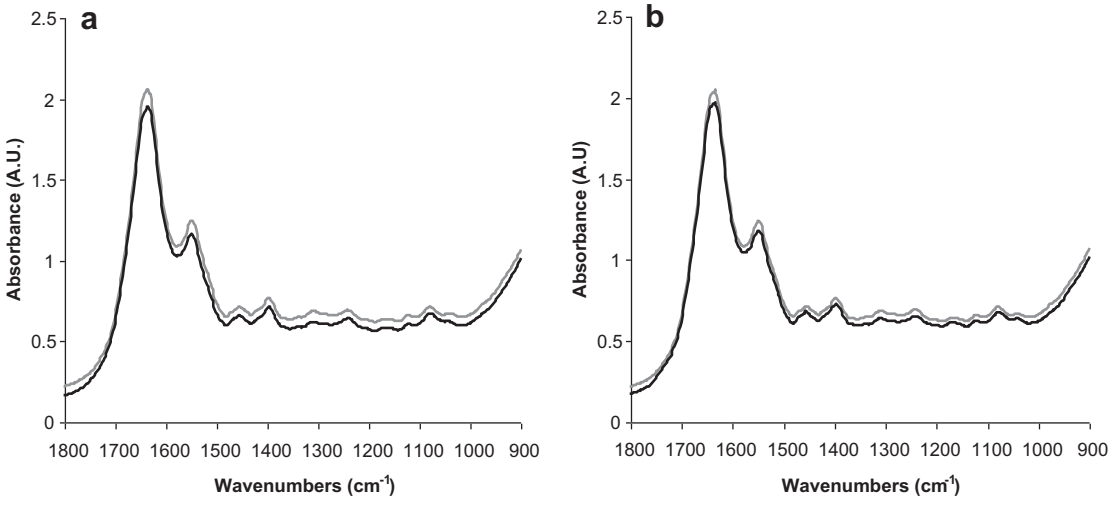

Fig. 2. Raw FT-IR spectra collected from minced beef samples stored aerobically (a) and under MAP (b) at 5 °C for 0 h: grey line and 144 h: black line.

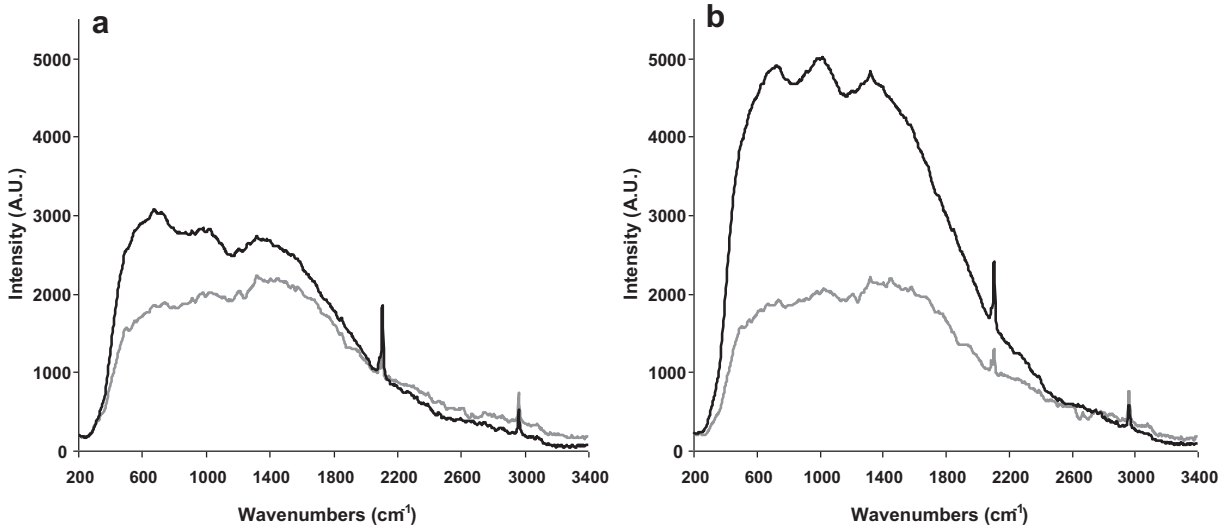

Fig. 3. Raw Raman spectra collected from minced beef samples stored aerobically (a) and under MAP (b) at 5 °C for 0 h: grey line and 144 h: black line.

Table 2
Root mean square errors for the validation estimates for each FT-IR and Raman model.

	Model	TVC	Pseudomonads	LAB	*Br. thermosphacta*	*Enterobacteriaceae*	Yeasts & Moulds	Sensory
FT-IR	PLS	0.5472 (9[a])	0.6007 (9)	0.4368 (9)	0.6886 (9)	0.4442(4)	0.5478(7)	0.3937(9)
	SVR_L	0.5040	0.5662	0.4162	0.7846	0.4345	0.5516	0.3932
	SVR_R	0.5109	0.5793	0.4111	0.6849	0.4382	0.5154	0.3941
	SVR_P	0.5098	0.5648	0.4153	0.6842	0.4394	0.5475	0.3908
	GA-ANN	0.7909	0.7845	0.5857	0.9914	0.4835	0.5683	0.6499
	GA-GP	43.8596	0.6375	0.5740	0.7635	0.4205	0.5807	0.3450
Raman	PLS	0.6301 (6)	0.8122 (3)	0.5513 (6)	0.7280 (6)	0.5245 (9)	0.6789 (5)	0.3228 (6)
	SVR_L	0.6777	0.8494	0.5328	0.8269	0.6502	0.3445	0.3932
	SVR_R	0.5629	0.7060	0.4626	0.7054	0.4961	0.6291	0.3277
	SVR_P	0.5713	0.7252	0.5107	0.7245	0.4345	0.5516	0.3932
	GA-ANN	0.9954	1.1708	0.6421	0.7905	0.7050	0.7907	0.3352
	GA-GP	1.0419	9.4335	0.6465	1.3131	0.8000	8.3899	0.7657

[a] Number of latent variables used to calculate the PLS model. SVR_L = linear. SVR_R = radial basis function. SVR_P = polynomial.

predictions were obtained for TVC, LAB and *Enterobacteriaceae*, whilst the FT-IR models performed in general slightly better in predicting the microbial counts compared to the Raman models. Additionally, regarding the predictions of the microbial counts the multivariate methods (SVM, PLS) that had similar performances gave better predictions compared to the evolutionary ones (GA-GP, GA-ANN, GP). This may arise from the fact that the stochastic nature of the later methods may make them unreliable for small data sets like those used here, with GA-GP particularly prone to 'over-fit' the data. On the other hand, the GA-GP model performed better than the others in predicting the sensory scores using the FT-IR data, whilst the GA-ANN model performed better in predicting the sensory scores using the Raman data.

It has to be mentioned, that it was hard to identify bands that were widely used as inputs by the GA-ANN and GA-GP methods. Only the basic GPs consistently used inputs within particular bands more than those elsewhere, for at least some of the predictions. For GP Raman models, the bands that were mostly used were from 2096 to 2140 cm^{-1} and from 3296 to 3400 cm^{-1} for all the cases. These frequencies could be assigned to free amino acids (NH_3^+ stretch) for the area observed in the spectra between 2141 and 1997 cm^{-1} (numerous peaks), to amines (N–H stretch)/ peracids (O–H stretch) for the area 3284–3250 cm^{-1} (peaks observed at 3275 and 3261), to amino acids/proteins/amines (NH stretch) for the area 3309–3291 cm^{-1} (peak at 3300), to amido acids/amino acids/ carbohydrates/polypeptides/amines (NH stretch)/water/lipids (OH stretch) for the area 3397–3309 cm^{-1} (numerous peaks) (Socrates, 2001; Yang & Irudayaraj, 2003). For the GP FT-IR models the most selected inputs were from 1132 to 1207 cm^{-1} for the TVC, *Pseudomonas* spp., yeasts and moulds and *Enterobacteriaceae*. These frequencies could be assigned to amide III (30% C–N stretch, 30% N–H bend, 10% C=O–N bend, 20% other)/ amines (C–N stretch) for the area 1211–1199 cm^{-1} (shoulder at 1205), to amines $-N(CH_3)_2$ (CH_3 rock and asymetric CCN stretch) for the area 1200–1190 cm^{-1} (shoulder at 1196), to fat (C–O stretch)/ esters (C–O–C)/carbohydrates (C–O stretch)/$-NH_2$ deformation for the area 1185–1143 cm^{-1} (double peak at 1165) (Böcker et al., 2007; Chen, Irudayaraj, & Mcmahon, 1998; Pappas et al., 2008; Socrates, 2001). The basic GP models and the SVR_S performed worse than the other SVR, GA-GP and GA-ANN models (i.e. they exhibited big RMSE for both FT-IR and Raman data) and the results will not be further analysed for these two models.

Regarding the FT-IR models, no particular trend of over- or under-prediction was observed, except from estimates of the yeasts and moulds that were always under-predicted irrespective of the model, the *Br. thermosphacta* that showed a trend of over-prediction in the case of PLS and the TVC that showed a trend of under-prediction in the case of GA-GP respectively. For the Raman models, a trend of under-prediction of all the counts was observed especially at bigger microbial loads in some cases, which was more intense at the predictions of yeasts and moulds.

Indicatively, Figs. 4 and 5 show the residuals for the prediction cases of TVC, pseudomonads and LAB for FT-IR SVR_L model and for the Raman SVR_R model respectively. The line $y = 0.5$ determines the fail-dangerous zone direction, whilst the line $y = -1.0$ determines the fail-safe zone (Oscar, 2009). Table 4 depicts the % PE values of the models, indicates that for FT-IR models, PLS, SVR_L and SVR_P gave for all the counts acceptable predictions (% PE > 70%), except from the counts of yeasts and moulds that were underestimated and were totally outside the acceptable range, no matter the model

Table 3
R^2 for the validation estimates for each FT-IR and Raman model.

	Model	TVC	Pseudomonads	LAB	*Br. thermosphacta*	*Enterobacteriaceae*	Yeasts & Moulds	Sensory
FT-IR	PLS	0.8066	0.7885	0.8392	0.7269	0.7562	0.7172	0.6453
	SVR_L	0.8368	0.8129	0.8163	0.6693	0.7740	0.7240	0.6660
	SVR_R	0.8316	0.8036	0.8178	0.7329	0.7600	0.7629	0.6580
	SVR_P	0.8329	0.8147	0.8167	0.7347	0.7682	0.7201	0.6659
	GA-ANN	0.7086	0.6504	0.6920	0.5313	0.7466	0.7654	0.5533
	GA-GP	0.0086	0.7656	0.6730	0.6670	0.7902	0.7101	0.7346
Raman	PLS	0.7259	0.5183	0.7449	0.7142	0.7169	0.6169	0.7834
	SVR_L	0.7205	0.5940	0.7220	0.6856	0.6068	0.7531	0.6660
	SVR_R	0.7951	0.7003	0.7874	0.7317	0.7232	0.6254	0.7781
	SVR_P	0.7893	0.6835	0.7649	0.7333	0.7740	0.7240	0.6660
	GA-ANN	0.4779	0.2894	0.6206	0.7035	0.4774	0.4341	0.8246
	GA-GP	0.3457	0.0018	0.6218	0.2697	0.3191	0.0045	0.2766

SVR_L = linear. SVR_R = radial basis function. SVR_P = polynomial.

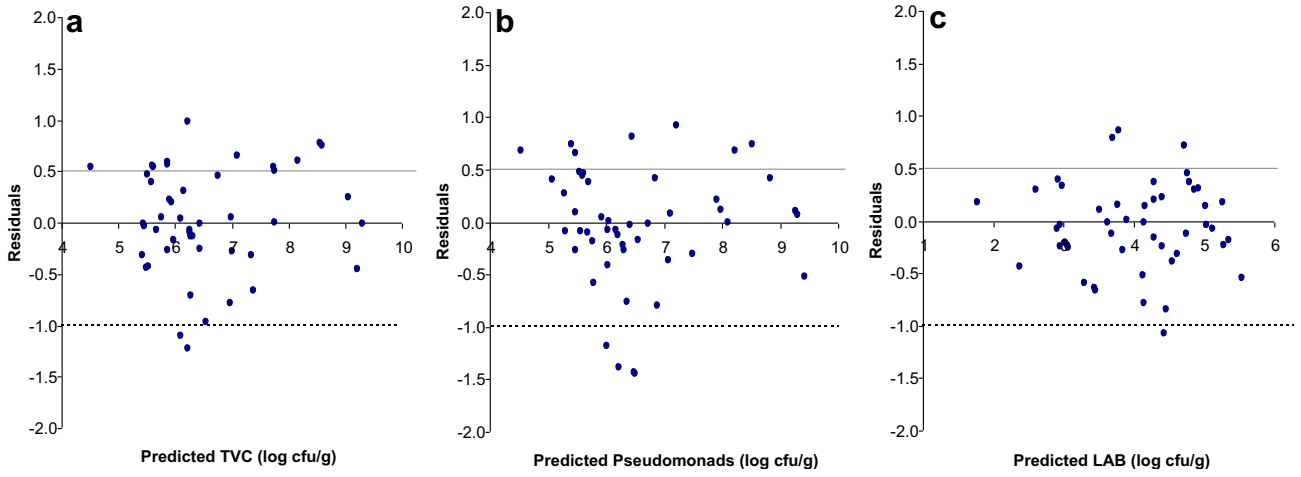

Fig. 4. Residuals vs. predicted values of the TVC (a), pseudomonads (b) and LAB (c) as estimated from the FT-IR SVR_L model. The dashed horizontal lines represent the acceptable prediction zone (APZ) (Oscar, 2009).

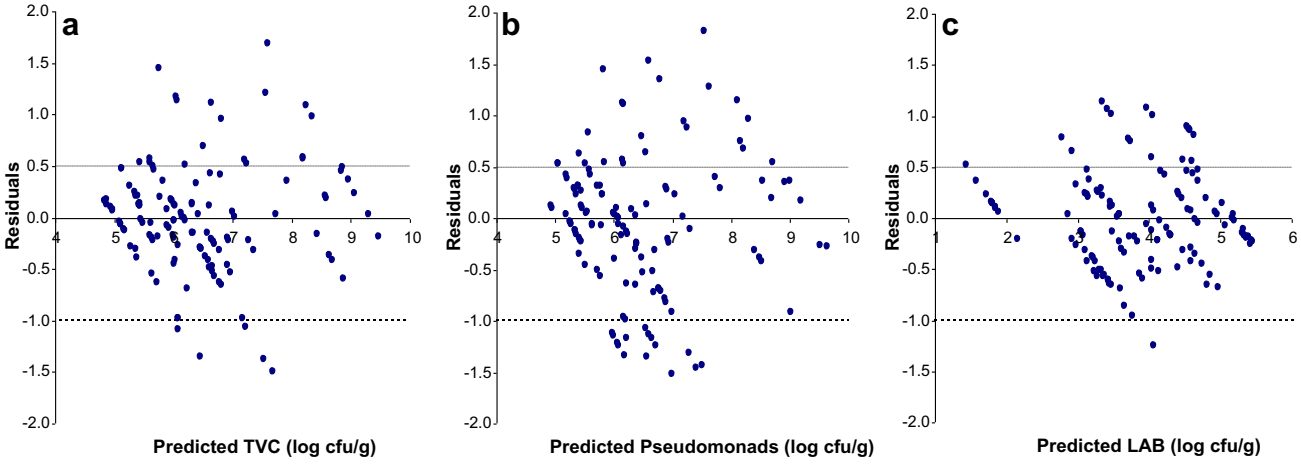

Fig. 5. Residuals vs. predicted values of the TVC (a), pseudomonads (b) and LAB (c) as estimated from the Raman SVR_R model. The dashed horizontal lines represent the acceptable prediction zone (APZ) (Oscar, 2009).

Table 4
Percentage of prediction error (% PE) for the validation estimates for each FT-IR and Raman model.

	Model	TVC	Pseudomonads	LAB	*Br. thermosphacta*	*Enterobacteriaceae*	Yeasts & Moulds
FT-IR	PLS	83.33	77.08	87.50	70.83	89.58	0.00
	SVR_L	83.33	83.33	95.83	83.33	85.42	0.00
	SVR_R	81.25	77.08	93.75	68.75	87.50	0.00
	SVR_P	87.50	79.17	81.25	77.08	83.33	0.00
	GA-ANN	66.67	62.50	81.25	60.42	95.83	0.00
	GA-GP	52.08	79.17	89.58	70.83	89.58	0.00
Raman	PLS	78.46	66.15	80.77	79.23	83.85	69.23
	SVR_L	81.54	63.85	82.31	66.92	85.38	82.31
	SVR_R	87.69	81.54	86.15	76.92	87.69	79.23
	SVR_P	86.92	70.77	86.15	82.31	89.23	81.54
	GA-ANN	64.62	54.62	76.15	66.92	73.85	71.54
	GA-GP	63.85	50.77	75.38	70.00	76.92	66.15

Table 5
Percentage of the correct classification of the validation sensory estimates for the FT-IR and Raman models.

	Class	Correct Classification (%)					
		PLS	SVR_L	SVR_R	SVR_P	GA-ANN	GA-GP
FT-IR	Fresh ($n=6$)	33.33	16.67	33.33	33.33	66.67	**66.67**
	Semi-fresh ($n=12$)	83.33	91.67	100.00	100.00	50.00	**91.67**
	Spoiled ($n=30$)	90.00	93.33	93.33	93.33	96.67	**90.00**
	Total ($n=48$)	81.25	83.33	87.50	87.50	81.25	**87.50**
Raman	Fresh ($n=26$)	80.77	73.08	69.23	73.08	**96.15**	23.08
	Semi-fresh ($n=30$)	56.67	70.00	66.67	80.00	**76.67**	73.33
	Spoiled ($n=74$)	90.54	90.54	87.84	90.54	**81.08**	87.84
	Total ($n=130$)	80.77	82.31	79.23	84.62	**83.08**	71.54

Table 6a
Confusion matrix of the GA-GP FT-IR model for the validation sensory estimates.

True class	Predicted class			Correct Classification (Sensitivity %)
	Fresh	Semi-fresh	Spoiled	
Fresh ($n=6$)	4	0	2	66.67
Semi-fresh ($n=12$)	0	11	1	91.67
Spoiled ($n=30$)	0	3	27	90.00
Total ($n=48$)	4	14	30	87.50
Specificity (%)	100.00	78.57	90.00	

Table 6b
Confusion matrix of the GA-ANN FT-IR model for the validation sensory estimates.

True class	Predicted class			Correct Classification (Sensitivity %)
	Fresh	Semi-fresh	Spoiled	
Fresh ($n=6$)	25	1	0	96.15
Semi-fresh ($n=30$)	5	23	2	76.67
Spoiled ($n=74$)	0	14	60	81.08
Total ($n=130$)	30	38	62	83.08
Specificity (%)	83.33	60.53	96.77	

used. For Raman models, SVR_R and SVR_P gave acceptable predictions (% PE > 70%) for all of the counts.

The classification accuracies of the sensory estimates regarding the FT-IR and Raman models for each class and in total can be seen at Table 5. As stated above, the evolutionary methods performed better than the others in predicting the sensory scores. Regarding the FT-IR data the GA-GP model gave an overall performance of 87.5% correct classification like the SVR_R and SVR_P, but the former gave better predictions concerning the correct classification of the fresh samples (Table 6a). In the case of the Raman spectra, the GA-ANN gave better results considering the fact that no fresh sample was misclassified as spoiled and *vice versa* (Table 6b).

4. Conclusions

The enormous amount of molecularly specific information provided by FT-IR and Raman spectroscopies make the data produced unmanageable to simple 'stare and compare' interpretation. Thus it is necessary to apply advanced multivariate statistical methods (*viz*., discriminant function analysis, clustering algorithms, chemometrics) and intelligent machine learning methodologies (*viz*., neural networks, fuzzy logic, evolutionary algorithms and genetic programming) for analysis. A subset of these algorithms were assessed in this study and we implemented these as qualitative and quantitative indices (Goodacre, Vaidyanathan, Dunn, Harrigan, & Kell, 2004).

We found that in particular the machine learning methods gave better predictions for all indices for the various bacterial and eukaryotic groups. We believe that these computational approaches could soon be used to implement the evaluation of meat spoilage. The results of this study demonstrate for the first time that Raman spectroscopy as well as FT-IR spectroscopy can be used reliably and accurately to the rapid assessment of meat spoilage. However, further studies are required to create databases and apply the appropriate prediction models, so that these methods can be applied within meat industries.

Acknowledgements

This work was supported by the EU Project Symbiosis-EU (no 211638) under the 7th Framework Programme for RTD. The information in this document reflects only the authors' views and the Community is not liable for any use that may be made of the information contained therein.

References

Al-Jowder, O., Defernez, M., Kemsley, E. K., & Wilson, R. H. (1999). Mid-infrared spectroscopy and chemometrics for the authentication of meat products. *Journal of Agricultural and Food Chemistry, 47*, 3210–3218.
Al-Jowder, O., Kemsley, E. K., & Wilsonb, R. H. (1997). Mid-infrared spectroscopy and authenticity problems in selected meats: a feasibility study. *Food Chemistry, 59*, 195–201.
Ammor, M., Argyri, A., & Nychas, G.-J. (2009). Rapid monitoring of the spoilage of minced beef stored under conventionally and active packaging conditions using Fourier transform infrared spectroscopy in tandem with chemometrics. *Meat Science, 81*, 507–515.
Argyri, A. A., Jarvis, R. M., Wedge, D., Xu, Y., Panagou, E., Goodacre, R., et al. (2011). A comparison of Raman and FTIR spectroscopy for the prediction of meat spoilage. In E. Cummins, J. M. Frias, & V. P. Valdramidis (Eds.), *Seventh international conference on predictive modelling in foods – Conference proceedings* (pp. 158–161). Dublin, Ireland: UCD, DIT, Teagasc.
Argyri, A. A., Panagou, E. Z., Tarantilis, P. A., Polysiou, M., & Nychas, G.-J. E. (2010). Rapid qualitative and quantitative detection of beef fillets spoilage based on Fourier transform infrared spectroscopy data and artificial neural networks. *Sensors and Actuators B, 145*, 146–154.
Baranyi, J., & Roberts, T. A. (1994). A dynamic approach to predicting bacterial growth in food. *International Journal of Food Microbiology, 23*, 277–294.
Beattie, R. J., Bell, S. J., Farmer, L. J., Moss, B. W., & Desmond, P. D. (2004). Preliminary investigation of the application of Raman spectroscopy to the prediction of the sensory quality of beef silverside. *Meat Science, 66*, 903–913.
Blanco, M., & Pages, J. (2002). Classification and quantitation of finishing oils by near infrared spectroscopy. *Analytica Chemica Acta, 463*, 295–303.
Böcker, U., Ofstad, R., Wu, Z., Bertram, H. C., Sockalingum, G. D., Manfait, M., et al. (2007). Revealing covariance structures in Fourier transform infrared and Raman microspectroscopy spectra: a study on pork muscle fiber tissue subjected to different processing parameters. *Applied Spectroscopy, 61*, 1032–1039.
Borch, E., Kant-Muemans, M.-L., & Blixt, Y. (1996). Bacterial spoilage of meat products. *International Journal of Food Microbiology, 33*, 103–120.
Chen, M., Irudayaraj, J., & Mcmahon, D. J. (1998). Examination of full fat and reduced fat cheddar cheese during ripening by Fourier transform infrared spectroscopy. *Journal of Dairy Science, 81*, 2791–2797.
Despagne, F., Massart, D. L., & Chabot, P. (2000). Development of a robust calibration model for nonlinear in-line process data. *Analytical Chemistry, 72*, 1657–1665.
Ellis, D. I., Broadhurst, D., Clarke, S. J., & Goodacre, R. (2005). Rapid identification of closely related muscle foods by vibrational spectroscopy and machine learning. *Analyst, 130*, 1648–1654.
Ellis, D. I., Broadhurst, D. I., & Goodacre, R. (2004). Rapid and quantitative detection of the microbial spoilage of beef by Fourier transform infrared spectroscopy and machine learning. *Analytica Chimica Acta, 514*, 193–201.
Ellis, D. I., Broadhurst, D., Kell, D. B., Rowland, J. J., & Goodacre, R. (2002). Rapid and quantitative detection of the microbial spoilage of meat by Fourier transform infrared spectroscopy and machine learning. *Applied and Environmental Microbiology, 68*, 2822–2828.
Ellis, D. I., & Goodacre, R. (2001). Rapid and quantitative detection of the microbial spoilage of muscle foods: current status and future trends. *Trends in Food Science and Technology, 12*, 414–424.
Ercolini, D., Russo, F., Torrieri, E., Masi, P., & Villani, F. (2006). Changes in the spoilage-related microbiota of beef during refrigerated storage under different packaging conditions. *Applied and Environmental Microbiology, 72*, 4663–4671.
Ferentinos, K. P. (2005). Biological engineering applications of feedforward neural networks designed and parameterized by genetic algorithms. *Neural Networks, 18*(7), 934–950.

Gill, C. O., & Jeremiah, L. E. (1991). The storage life of non-muscle offals packaged under vacuum or carbon dioxide. *Food Microbiology, 8*, 339–353.
Goldberg, D. E. (1989). *Genetic algorithms in search optimization and machine learning*. Addison Wesley, ISBN 0201157675. p. 41.
Goodacre, R. (2005). Making sense of the metabolome using evolutionary computation: seeing the wood with the trees. *Journal of Experimental Botany, 56*, 245–254.
Goodacre, R., Vaidyanathan, S., Dunn, W. B., Harrigan, G. G., & Kell, D. B. (2004). Metabolomics by numbers: acquiring and understanding global metabolite data. *Trends in Biotechnology, 22*, 245–252.
Guo, Q., Wu, W., Questier, F., Massart, D. L., Boueon, C., & De Jong, S. (2000). Sequential projection pursuit using genetic algorithms for data mining of analytical data. *Analytical Chemistry, 72*, 2846–3285.
Haykin, S. (2009). *Neural networks and learning machines* (3rd ed.). NJ: Pearson Education.
Herrero, A. M. (2008a). Raman spectroscopy a promising technique for quality assessment of meat and fish: a review. *Food Chemistry, 107*, 1642–1651.
Herrero, A. M. (2008b). Raman spectroscopy for monitoring protein structure in muscle food systems. *Critical Reviews in Food Science and Nutrition, 48*, 512–523.
Herrero, A. M., Carmona, P., & Careche, M. (2004). Raman spectroscopic study of structural changes in hake (*Merluccius merluccius* L.) muscle proteins during frozen storage. *Journal of Agricultural and Food Chemistry, 52*, 2147–2153.
Karoui, R., Lefur, B., Grondin, C., Thomas, E., Demeulemester, C., De Baerdemaeker, Josse, et al. (2007). Mid-infrared spectroscopy as a new tool for the evaluation of fish freshness. *International Journal of Food Microbiology, 42*, 57–64.
van Kempen, T. (2001). Infrared technology in animal production. *Worlds Poultry Science Journal, 57*, 29–48.
Konoz, E., & Golmohammadi, H. (2008). Prediction of air-to-blood partition coefficients of volatile organic compounds using genetic algorithm and artificial neural network. *Analytica Chemica Acta, 619*, 157–164.
Koza, J. (1992). *Genetic programming: On the programming of computers by means of natural selection*. MIT Press.
McMeekin, T. A., Baranyi, J., Bowman, J., Dalgaard, P., Kirk, M., Ross, T., et al. (2006). Information systems in food safety management. *International Journal of Food Microbiology, 112*, 181–194.
McMeekin, T. A., Mellefont, L. A., & Ross, T. (2007). Predictive microbiology; past present and future. In S. Brul, S. van Gerwen, & M. Zwietering (Eds.), *Modelling microorganisms in food* (pp. 7–21). Cambridge: Woodhead.
Marquardt, B. J., & Wold., J. P. (2004). Raman analysis of fish: a potential method for rapid quality screening. *Lebensmittel-Wissenschaft und Technologie, 37*, 1–8.
Nicolaou, N., & Goodacre, R. (2008). Rapid and quantitative detection of the microbial spoilage in milk using Fourier transform infrared spectroscopy and chemometrics. *Analyst, 133*(10), 1424–1431.
Nicolaou, N., Xu, Y., & Goodacre, R. (2011). Fourier transform infrared and Raman spectroscopies for the rapid detection, enumeration, and growth interaction of the bacteria *Staphylococcus aureus* and *Lactococcus lactis* ssp. *cremoris* in milk. *Analytical Chemistry, 83*(14), 5681–5687.
Nychas, G. J. E., Drosinos, E., & Board, R. G. (1998). Chemical changes in stored meat. In R. G. Board, & A. R. Davies (Eds.), *The microbiology of meat and poultry* (pp. 288–326). London: Blackie Academic and Professional.
Nychas, G.-J. E., Skandamis, P. N., Tassou, C. C., & Koutsoumanis, K. P. (2008). Meat spoilage during distribution. *Meat Science, 78*, 77–89.
Oscar, T. P. (2005). Validation of lag time and growth rate models for *Salmonella Typhimurium*: acceptable prediction zone method. *Journal of Food Science, 70*, 129–137.
Oscar, T. P. (2009). Predictive model for survival and growth of *Salmonella Typhimurium* DT104 on chicken skin during temperature abuse. *Journal of Food Protection, 72*, 304–314.
Papadopoulou, O., Panagou, E. Z., Tassou, C. C., & Nychas, G.-J. E. (2011). Contribution of Fourier transform infrared (FTIR) spectroscopy data on the quantitative determination of minced pork meat spoilage. *Food Research International, 44*(10), 3264–3271.
Pappas, C. S., Tarantilis, P. A., Moschopoulou, E., Moatsou, G., Kandarakis, I., & Polissiou, M. G. (2008). Identification and differentiation of goat and sheep milk based on diffuse reflectance infrared Fourier transform spectroscopy (DRIFTS) using cluster analysis. *Food Chemistry, 106*, 1271–1277.
Sakala, R. M., Hayashidani, H., Kato, Y., Hirata, T., Makino, Y., Fukushima, A., et al. (2002). Change in the composition of the microflora on vacuum packaged beef during chiller storage. *International Journal of Food Microbiology, 74*, 87–99.
Shinoda, K., Sugimoto, M., Tomita, M., & Ishihama, Y. (2008). Informatics for peptide retention properties in proteomic LC-MS. *Proteomics, 8*, 787–798.
Skandamis, P. N., & Nychas, G.-J. E. (2001). Effect of oregano essential oil on microbiological and physico-chemical attributes of minced meat stored in air and modified atmospheres. *Journal of Applied Microbiology, 91*, 1011–1022.
Skandamis, P. N., & Nychas, G.-J. E. (2002). Preservation of fresh meat with active and modified atmosphere packaging conditions. *International Journal of Food Microbiology, 79*, 35–45.
Smola, A. J., & Schölkopf, B. (2004). A tutorial on support vector regression. *Statistics and Computing, 14*, 199–222.
Socrates, G. (2001). *Infrared and Raman characteristic group frequencies* (3rd ed.). West Sussex, UK: John Willey & Sons Ltd Press.
Sowoidnich, K., Schmidt, H., Maiwald, M., Sumpf, B., & Kronfeldt, H.-D. (2010). Application of diode-laser Raman spectroscopy for in situ investigation of meat spoilage. *Food Bioprocess Technol, 3*, 878–882.
Tang, K., & Li, T. (2002). Combining PLS with GA-GP for QSAR. *Chemometrics and Intelligent Laboratory Systems, 64*, 55–64.
Thissen, U., Ustun, B., Melssen, W. J., & Buydens, L. M. C. (2004). Multivariate calibration with least-squares support vector machines. *Analytical Chemistry, 76*, 3099–3105.
Torres, M., Hervás, C., & Amador, F. (2005). Approximating the sheep milk production curve through the use of artificial neural networks and genetic algorithms. *Computers & Operations Research, 32*, 2653–2670.
Tsigarida, E., Skandamis, P. N., & Nychas, G.-J. E. (2000). Behaviour of *Listeria monocytogenes* and autochthonous flora on meat stored under aerobic, vacuum and modified atmosphere packaging conditions with or without the presence of oregano essential oil at 5 °C. *Journal of Applied Microbiology, 89*, 901–909.
Vapnik, V. (1995). *The nature of statistical learning theory*. New York: Springer.
Yang, H., & Irudayaraj, J. (2001). Characterization of beef and pork using Fourier-transform infrared photoacoustic spectroscopy. *LWT – Food Science and Technology, 34*, 402–409.
Yang, H., & Irudayaraj, J. (2003). Rapid detection of foodborne microorganisms on food surface using Fourier transform Raman spectroscopy. *Journal of Molecular Structure, 646*(1–3), 35–43.
Zou, T., Dou, Y., Mi, H., Zou, J., & Ren, Y. (2006). Support vector regression for determination of component of compound oxytetracycline powder on near-infrared spectroscopy. *Analytical Biochemistry, 355*, 1–7.